# Control System for the automatic Handling of biological Cells with mobile Microrobots

Helge Hülsen
helge.huelsen@informatik.uni-oldenburg.de

Tammo Trüper
tammo.trueper@informatik.uni-oldenburg.de

Sergej Fatikow
fatikow@uni-oldenburg.de

Division Microrobotics and Control Engineering
University of Oldenburg
26111 Oldenburg, Germany

***Abstract* – This paper describes current research activities on the development of a control system for the automated handling of biological cells with mobile microrobots. Two main aspects are covered: A motorized inverted microscope is used to extract position coordinates of the microrobot's end-effector and the biological objects. A motion control system uses this sensor information to move a mobile microrobot with high precision on the microscope's stage. This system can then be used to automatically transport biological cells to different repositories or to perform microdissection.**

## I. INTRODUCTION

Handling of biological microobjects is becoming increasingly important in such diverse fields as medical research, biotechnology, genetics and biological research. With increasing interest in micromanipulation the necessary tools, especially manipulators and end-effectors have become more and more sophisticated and mature (see e.g. [1]). Also the tools for visualisation and optical sensoring continuously improve, for example in near field optical microscopy or 3D-fluorescence. Still, many tasks are being performed with regular brightfield microscopy, which is technologically mature.

The interpretation of the sensory data – the mircroscope image – is not highly automatized. This means the link between the sensor, i.e. the microscope, and the actuator is established by the human operator via visual inspection on one side and control of the microscope and tele-operation of the manipulator on the other side. This work is tedious but, at the same time, requires highly trained operators. The aim of the research presented in this paper is to close the gap between sensor and actuator and to provide tools towards a higher degree of automation of the handling of biological microobjects under optical microscopes. The control system of the actuators has been especially designed with respect to the problems at the micrometer and sub-micrometer scale: Non-linearities, time-variance and complex mathematical models of the actuators' behaviour.

In section II, the general system set-up with the microrobots will be described. Section III presents the control of the microscope, which is used as a sensor for the motion control system in section IV, which covers the control system architecture as well as the control methods used for tele-operated and automatic handling of biological cells. Experimental results are given in section V. The paper is concluded in section VI.

## II. SET-UP

### *A. End-Effectors*

A motorized inverted microscope with digital cameras, machine vision and image processing provides the primary sensor system of the microhandling station. There is a variety of end-effector types for the handling of living cells. To avoid damage to the cells, mechanical contact should be minimised. Furthermore, it is important that the field of vision is not obscured by the end-effector. The most popular approach of non-contact manipulation is laser trapping [2,3,4] but the necessarily high laser power for holding a live cell bears the danger of damaging the it. In addition the optical trapping system is fixed to the microscope's optical system for beam focussing and can therefore not be used flexibly. Using dielectrophoresis or electrorotation [4,5] is another non-contact approach but the achieved forces are too small to hold the cell for purposes like microinjection. For applications like this, cells are hold and manipulated mechanically by glass capillaries, which offer a good compromise between transparency and visibility needed to gather position information.

### *B. Mobile Microrobot*

Commercial manipulators available today have several limitations with respect to their flexibility. Many manipulation systems are specialised towards one application and are not built in a modular manner. In addition many of them are physically fixed to a microscope, sometimes requiring extensive retrofitting of the microscope. To avoid these problems, a mobile microrobot has been built [6]. It consists of three main parts, a mobile platform, a manipulation unit and end-effectors (Fig. 1). The mobile microrobot's platform, which is based on piezo-electric actuators, is able to move with three DOF on a stage of an inverted microscope. The stage's size is the only limitation on the working space.

Due to the modular concept different manipulation units with different configurations can be attached to the mobile platform. This can range from a simple piezo-stack with one DOF to Gough-Stewart platforms with six DOF. The choice of the manipulation unit depends on which positioning accuracy is required by the application. The application specific end-effector is finally plugged into the manipulator's arm. In experiments described in this paper a standard capillary for cell holding was used with a CellTram microinjector (Eppendorf).

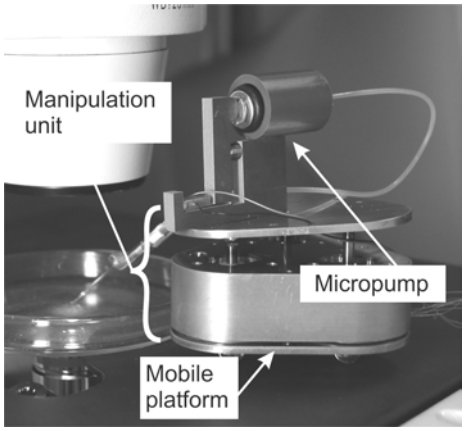

Fig. 1: Microrobot with integrated micropump.

## III. SENSOR CONTROL

### *A. Microscope and Imaging*

The microscope used for these experiments was a Zeiss Axiovert 200M inverted motorized microscope without special modifications. For image acquisition a digital CCD color camera (Basler A101fc) was used. The control software for the microscope was written in our group, which was necessary because of the tight integration of the microscope control into the whole control concept of the micromanipulation process. Image processing routines from the Matrox Imaging Library (MIL) were used.

### *B. Determining Positions*

The robots presented in this paper have no internal position sensors. That means that for the robots as well as for the cells the microscope image is the primary source of information available for control purposes. Thus, image processing is mandatory for position measurements. The coordinate system for the experiments is defined so that the microscope stage is the x-y-plane and the z-coordinate is normal to that plane and parallel to the movement of the focus drive. The focus drive has a built-in sensor for its position, this sensor is used to gain information about the z-coordinates of target objects as well as the robot's end-effector. The microscope's focus drive controller has a sufficient resolution with a minimum step size of 0.025 µm (manufacturer's specification).

Detecting a position can be separated into two tasks: detecting the z-position of the object, and detecting the object in the x-y-plane for that z-position. Since the target objects (cells) can be expected to not change their z-position without manipulation, the z-position of the object focus plane can be detected at the beginning of the experiment by scanning the focus drive range and measuring the focus index determined by a regular auto-focus algorithm that detects and correlates edges in the image.

In the object focus plane, a geometric model finder algorithm could be used to detect and track the target object. For these experiments Expancel spheres were used – transparent polymer spheres encapsulating a gas which can be expanded to various diameters across the range of typical mammalian cells by applying heat. At the beginning of a manipulation experiment, the microrobot will enter the microscope's area of view with the end-effector – the capillary – at a height reasonably far above the focus plane of the objects to prevent damaging the delicate tip of the capillary. The z-position of the capillary can be found by the focus scan mentioned above at the beginning of the experiment. The result of the focus scan procedure is shown in Fig. 2. It yields two distinct focus peaks, one representing the object plane and the other the z-position of the capillary.

Lowering the capillary to the object plane causes the two distinct focus peaks to merge into one broader peak, so that the capillary position cannot be reliably detected anymore by the focus scan method. Also, it is necessary that the microscope's focus follows the end-effector during the experiment, to provide a continuous stream of z-position measurements which is necessary for closed loop control of the end-effector's position.

Thus, after having found the z-position of the capillary at the beginning of the experiment, a new strategy to follow the capillary with the microscope's focus is used. For this, a geometrical model finder (GMF) algorithm is used. This algorithm detects a geometrical reference shape – the end-effector's tip – in the image, and puts out four values: x- and y-position, the angle φ (rotation in the x-y-plane), and a correlation value called "score". This score value is essentially useful in implementing a Focus-Follower algorithm. As shown in Fig. 3, the score depends on the sharpness of the capillary in the image. This way, it can be used for object-specific auto-focusing: disregarding the focus quality of all other objects in the image, the GMF score is sensitive to the sharpness of the capillary alone, while the GMF at the same time delivers the information necessary for closed-loop position control in the x-y-pla

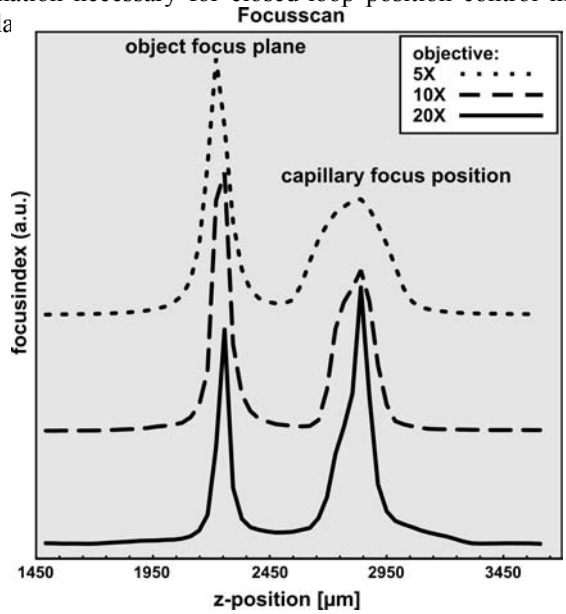

Fig. 2: Focusscan with different objectives; normalized. Notice that the peaks are narrowing for greater magnification – smaller depth of focus.

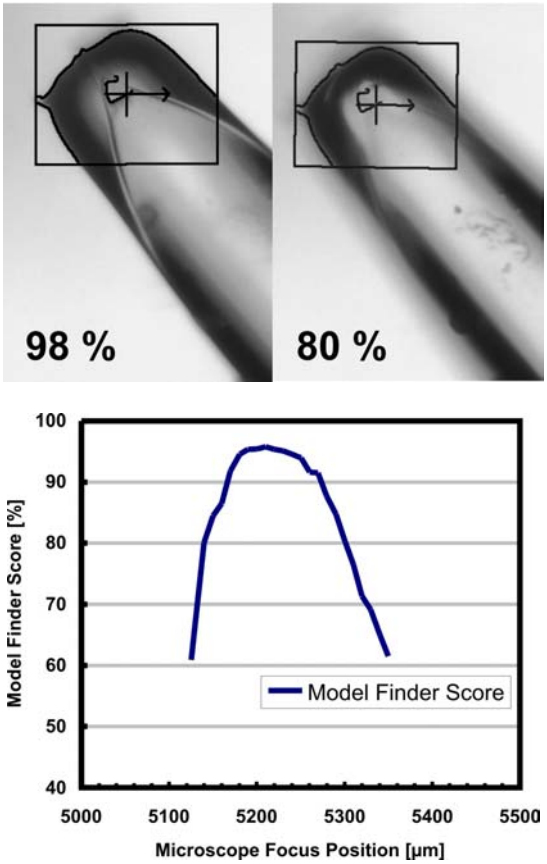


Fig. 3: Capillary in focus (top left), slightly out of focus (top right). Numbers ("score") reflect the correlation between the original model used by the geometrical model finder algorithm and the actual image. The graph shows the relation between the score and the microscope's focus position.

By implementing a closed-loop control for the focus drive, the image is continuously auto-focused exclusively to the capillary tip. Running independently from the motion control of the robot, this control loop delivers the z-position of the capillary – that means this control loop ranks hierarchically lower than the overall motion control loop and serves that loop as a sensor.

In this concept, the small depth of focus of typical microscope images is actually an advantage for z-position measurement. The precision of the Focus-Follower increases with smaller depth of focus. This means, with the aid of the microscope's focus drive, we can extract four coordinates from a two-dimensional picture: x,y,z and φ.

## IV. MOTION CONTROL

### *A. Control System Architecture*

For the manual and automatic positioning of the mobile microrobot with help of the vision system the control system architecture in Fig. 4 is used. The open-loop control module calculates the parameters of the signals which control the movement of the platform and the manipulator in a certain direction with a certain velocity. The signals for the actuators of the manipulator and the platform are generated with multichannel digital-analog-converter boards and linear amplifiers. The position of the microrobot is tracked by the microscope and the image processing system as described before. This position is then used as input for the closed-loop control, which is either accomplished tele-operated by the user or automatically by the closed-loop control module.

### *B. Control Task*

For the application of transporting and sorting cells the control task is to move the end-effector to a certain *(x,y,z)*-position and to hold it there. In a first approach this control task is separated into the positioning on the *(x,y)*-plane and the positioning on the *z*-axis. This separation is possible with a constraint mentioned below since these subtasks have their dedicated sensors and actuators. Using the current manipulator a movement in *z*-direction often also causes the end-effector to change its *(x,y)*-position. The *z*-positioning must therefore be executed prior to the *(x, y)*-positioning. To control all axes of the *(x,y,z)*-position the *(x,y)*-position control and the *z*-position control had to be synchronized.

### *C. Open-Loop Control*

*z-position: T*he open-loop control of the end-effector's *z*-position is depending on the manipulation unit and typically not very difficult when disregarding the *x*- and *y*-position. For a piezo-stack-actuated manipulation unit, a voltage that is approximately proportional to the desired position is applied. The voltage-position relation can easily be measured although special attention must be given to the hysteresis.

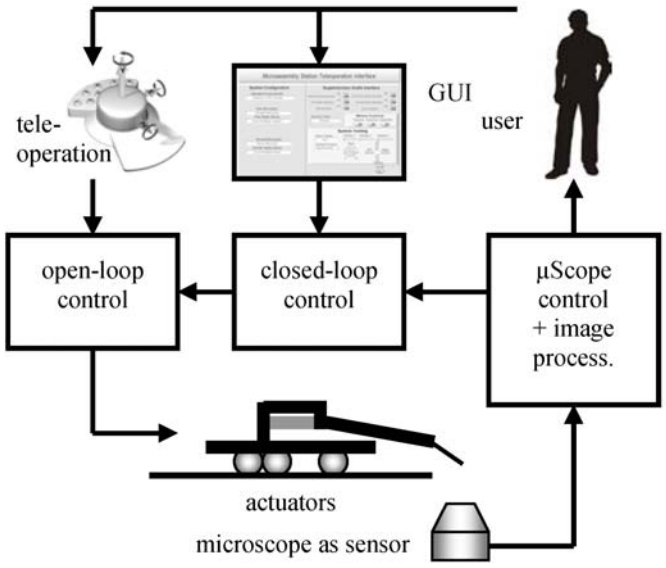


Fig. 4 Control system architecture.

*(x,y)-position:* For the open-loop control of the end-effector's measured position in world coordinates $\left[x_m^{(w)} \quad y_m^{(w)}\right]^T$, the desired position $\left[x_d^{(w)} \quad y_d^{(w)}\right]^T$, e.g. a point in front of the object's edge to be gripped, is first transformed into local, polar coordinates $\mathbf{g}_d = \left[r_d \quad \varphi_d\right]^T$, i.e. the distance and direction of that position is calculated in relation to the current position of the end-effector. The control algorithm must then perform the mapping from the desired position $\mathbf{g}_d$ to the corresponding amplitudes $\mathbf{p}_a = \left[v_1 \quad \ldots \quad v_6\right]^T$ of the signals, which are applied to the piezo actuators for a certain time to reach that position. Since the distance $r_d$ maps to the actuation parameters $\mathbf{p}_a$, which control the microrobot's velocity, updating the actuation parameters $\mathbf{p}_a$ frequently during the movement results in an implicit velocity control.

For finding the mapping $\mathbf{g}_d \rightarrow \mathbf{p}_a$ the following constraints must be kept in mind:

a) Experiments measuring the dependency of the microrobot's velocity from the control parameters have shown non-linear behaviour.
b) Because relevant physical relations and material constants are difficult to determine and due to coarse fabrication methods a corresponding mathematical model could only be obtained with high effort.
c) For the positioning of platforms and manipulators in the micrometer range the quality of the working surface and actuators, wear and changes of temperature or air humidity lead to time-variant parameters [6]. The controller should be able to adapt to these parameters during run-time.
d) The mapping from the desired direction and distance to the six amplitudes is under-determined and additional constraints like energy consumption are necessary.

The approach presented here is to empirically determine actuation parameters $\mathbf{p}_i$ that move the microrobot to certain local positions $\mathbf{g}_i$ that are ordered in a 2D grid, which does not necessarily need to be regular as in Fig. 5.

When a desired position $\mathbf{g}_d$ is given interpolation can be performed similar to algorithms in computer graphics or finite element analysis where blending functions define the weight $f_i$ of their support vectors $\mathbf{p}_i$ for the output vector $\mathbf{p}_a$:

$$\mathbf{p}_a = \sum_i f_i \cdot \mathbf{p}_i \tag{1}$$

To allow for a smooth transition between support vectors the sum of the blending factors $f_i$ shall not exceed 1:

$$f_i = \begin{cases} \dfrac{\tilde{f}_i}{\sum_k \tilde{f}_k} & \text{if } \sum_k \tilde{f}_k > 1 \\ \tilde{f}_i & \text{otherwise} \end{cases} \tag{2}$$

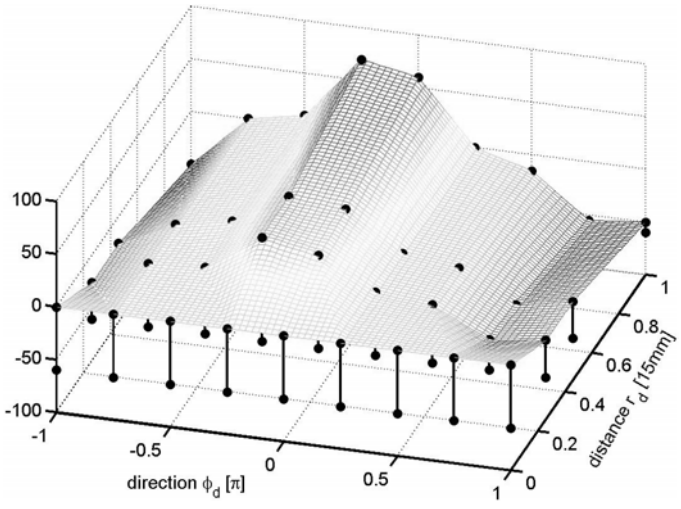

Fig. 5: Interpolation of support vectors for amplitude $v_6$

A blending factor $\tilde{f}_i$ is a measure of how close the desired position $\mathbf{g}_d$ is to the corresponding support vector $\mathbf{g}_i$. More specifically, each support vector $\mathbf{g}_i$ has a support range, which is limited by lines $j$ with position vector $\mathbf{g}_{pij}$ and line normal $\mathbf{n}_{pij}$. The requirement for each blending factor $\tilde{f}_i$ is that its value approaches 1 for all $\mathbf{g}_d$ which are close to $\mathbf{g}_i$ and 0 for all $\mathbf{g}_d$ which are close to the limiting lines as shown in Fig. 6 for $\tilde{f}_{12}(\mathbf{g}_d)$.

One solution is to use the minimum of all blending values $f_{ij}^{(p)}$ towards each limit $j$:

$$\tilde{f}_i = \min(f_{ij}^{(p)}) \tag{3}$$

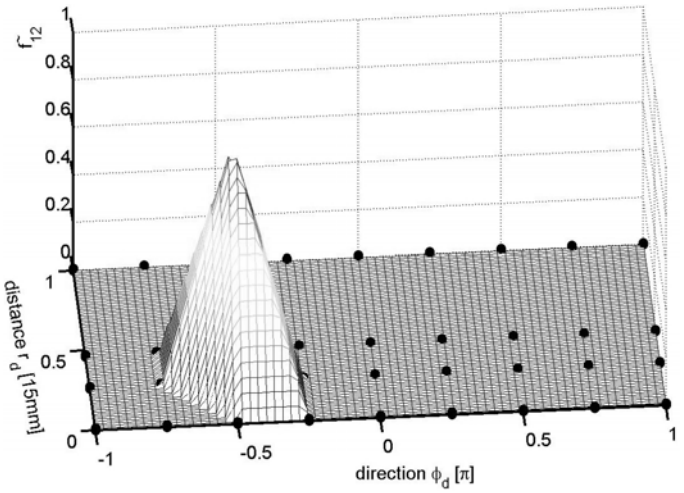

Fig. 6 Blending value $\tilde{f}_{12}$ for $\mathbf{g}_{12}$

These blending values can be calculated with help of:

$$f_{ij}^{(p)} = \begin{cases} 1 & \text{for } d_{ij} < 0 \\ 0 & \text{for } d_{ij} > 0 \\ 1 - d_{ij} & \text{otherwise} \end{cases}, \quad (4)$$

where $d_{ij}$ is the distance of $\mathbf{g}_d$ from $\mathbf{g}_i$ in the direction of the limit normal and scaled to its maximum value:

$$d_{ij} = \frac{d_{xij}}{d_{pij}} = \frac{\left|\mathbf{n}_{pij} \cdot (\mathbf{g}_d - \mathbf{g}_i)\right|}{\left|\mathbf{n}_{pij} \cdot (\mathbf{g}_{pij} - \mathbf{g}_i)\right|} \quad (5)$$

Seen from the fuzzy logic point of view (4) and (5) are the fuzzification operations, (3) is the conjunction of the different fuzzy values and (1) and (2) can be seen as the defuzzification operation.

For the definition of where and how limits are placed to limit the support vector's ranges the support vectors themselves are used. The limits of the range of a support vector are defined by combinations of adjacent support vectors. In Fig. 7 an arrangement of support vectors in a regular perpendicular grid with dimension 2 is presented. For each support vector, denoted by [0,0], a support range that is composed of triangles can be found. Its limits are defined by combinations of a subset of all adjacent support vectors, yielding 6 lines. For support vectors that lie at a border of the grid this number will be smaller.

The mapping $\mathbf{g}_d \rightarrow \mathbf{p}_a$ is initialised with empirical data in the current set-up and thus allows controlling a system with non-linear behaviour. In addition, this a-priori knowledge is used to avoid problems with ambiguities and mathematical models. The interpolation method has been designed to be adaptable to higher dimensions, where the limits are planes and hyper planes instead of lines. Furthermore it avoids the necessity for a regular input grid, such that the input support vectors $\mathbf{g}_i$ can be adapted to the distribution of desired positions $\mathbf{g}_d$. The interpolation is still easy enough to find adaptation algorithms also for the output support vectors $\mathbf{p}_i$. A promising approach is to extend the interpolation method by the Kohonen learning method [8][9].

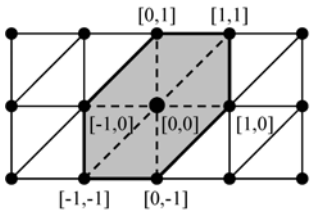


Fig. 7 Limiting vectors, lines and planes for a a) 1D grid and b) 2D grid

### *D. Closed-Loop Control*

For the closed-loop position control there are two different levels of automation that have been implemented (see Fig. 4). In a tele-operated mode three axes of a tele-operation device are assigned to the desired *z*-position and the desired *(x,y)*-position. The closed-loop control, i.e. the adjustment of the desired local position to reach a final position in world coordinates, is accomplished by the human operator. To allow for a more accurate control by the user after each sampling of the tele-operation device the microrobot is moving for a certain time, followed by a pause time.

In an automatic mode the targeted z-position and the targeted *(r,φ)*-position can be adjusted by the following algorithms: For the closed-loop control of the *z*-position the measured *z*-position from the focus scan algorithm or the correlation value from the object recognition algorithm can be input to a fuzzy controller which calculates the change of the desired z-position. For the closed-loop control of the *(x,y)*-position a first approach was to always use the current local desired position as input for the open-loop control. For a higher accuracy or higher velocity it may be necessary to take the dynamic of the microrobot into account. Furthermore, the implemented approach does not yet consider changes of the end-effector's orientation, which is tolerable in applications where the end-effector or the object to be manipulated is axially symmetric.

## V. EXPERIMENTS

To test the system's capability of handling cells a semi-automatic approaching has been carried out. In Fig. 8 pictures of a video are shown where the capillary is first moved laterally to its direction and then moved along its direction to approach the cell frontally. The desired trajectory is given by five support points with a desired accuracy of 10µm, denoted as circles with a corresponding diameter. Each of the pictures shows the position of the capillary at such a support point and the measured trajectory as dashed line. The cell can now be held pneumatically, transported to another position and released.

It can be seen that the robot reaches all five support points, although the measured trajectory is not always linear. The reason is that the microrobot is always heading the desired support point, which does not imply a linear trajectory. To avoid this problem, an on-line calculation of a trajectory could help, which would be a crucial requirement for microdissection of tissue.

These experiments show that the robot is capable of controlled, precise movement, so that cells can be successfully handled and transported. A complete manipulation task, namely approaching, holding, lifting, transporting, lowering and releasing, is shown in [10].

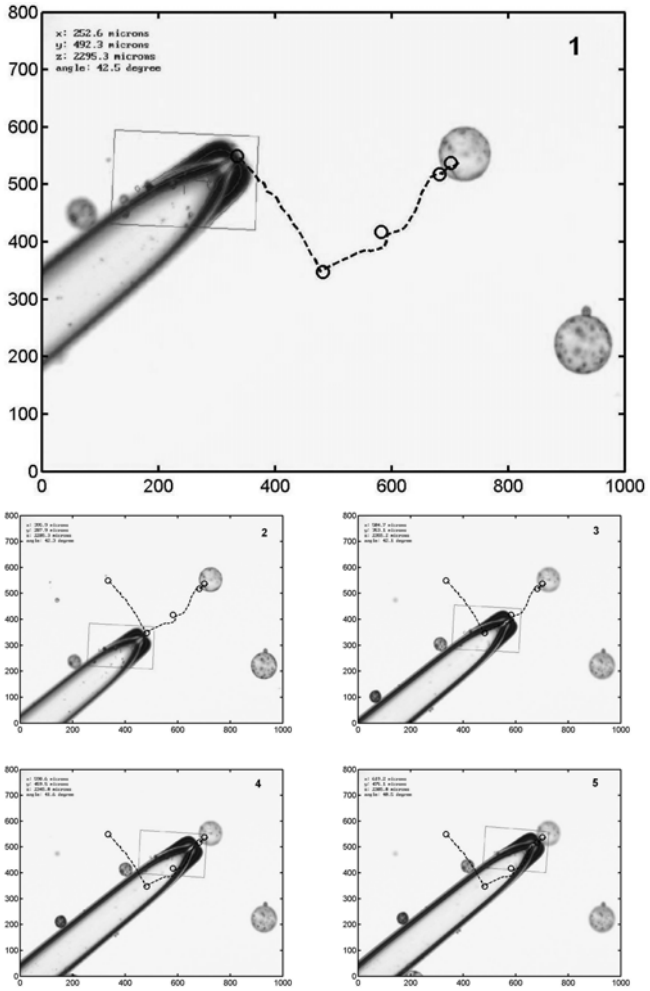


Fig. 8: A sequence of automatically approaching a cell with a capillary.

## VI. CONCLUSION

In this paper, a setup for the handling and transporting of cells has been presented. Different components have been developed: a mobile microrobot, an autofocusing system that consists of two different working modes for coarse and fine detection of the z-position of the end-effector, and a control system that can control the robot in tele-operated and automatic modes. The control system is divided into an open-loop control module and a closed-loop control module. For the open-loop control of the mobile platform a new fuzzy logic-based algorithm with the following features has been presented:

- Non-linearities of the microrobot's behaviour can be compensated.
- The design was carried out without a mathematical model of the microrobot's behaviour.
- Non-exact sensor information can be processed since the neighbourhood property ensures that similar inputs (desired poses) lead to similar outputs (parameters).
- The grid in the input space does not need to be regular, which allows to arbitrarily placing the input support vectors and gives more freedom for the description of the necessary control knowledge. This design also allows the extension by the Kohonen learning algorithm.

The experimental results show that the components of the whole system work together and make a smooth handling of a cell possible.

## VII. ACKNOWLEDGMENTS:

This paper is based on research supported by the European Union, the project ROBOSEM (GRD1-2001-41864). Financial support is gratefully acknowledged.

## VIII. REFERENCES

[1] Kleindiek Nanotechnik, " Micro Manipulator MM3A for Patch-Clamp", http://www.nanotechnik.com/

[2] Ashkin, A., "Acceleration and Trapping of Particles by Radiation Pressure", *in Phys. Rev. Letters*, vol. 24, No. 4, 1970, pp. 156-159.

[3] Conia, J., B.S. Edwards, S. Voelkel, "The Microrobotic Laboratory: Optical Trapping and Scissing for the Biologist", *in J. of Clinical Laboratory Analysis*, Vol. 11, No. 1, 1997, pp. 28-28.

[4] Ozkan, M., T. Pisanic, J. Sheel, C. Barrow, S. Esener and S. Bhatia, "Electro-Optical Platform for the Manipulation of Live Cells.", *in Special issue on the Biomolecular Interface*, Langmuir. 19(5); 2003, 1532-1538.

[5] Arai, F., K. Mosishima, T. Kasugai, T. Fukuda, "Bio-Micromanipulation (new direction for operation improvement)", *in Proc. IEEE/RSJ Int. Conf. on Intelligent Robot and Systems (IROS)*, 1997, pp. 1300 – 1305.

[6] Kortschack, A., A. Shirinov, T. Trüper, S. Fatikow, "Development of mobile versatile Nanohandling Microrobots: Design, Driving Principles, Haptic Control", J. ROBOTICA - *"A special issue on Micro/Nano Robotic Perception, Control and Manipulation"*, 2003.

[7] Zhou, Q., et al., "Environmental Influences on Microassembly", *in Proc. of IEEE/RSJ International Conference on Intelligent Robots and Systems (IROS)*, Lausanne, Switzerland, 2002.

[8] Ritter, H., T. Martinetz, K. Schulten, *Neural Computation and Self-Organizing Maps*, Addison-Wesley, Reading, Mass., 1992.

[9] Hülsen, H., St. Garnica, S. Fatikow, "Extended Kohonen Networks for the Pose Control of Microrobots in a Nanohandling Station", *in Proc. of the IEEE International Symposium on Intelligent Control (ISIC)*, Houston, Texas, USA, October 5-8, 2003.

[10] Trüper, T., A. Kortschack, M. Jähnisch, H. Hülsen, S. Fatikow: "Transporting and Sorting of Cells with Microrobots", *in Proc. of 2nd VDE World Microtechnologies Congress (MICRO.tec)*, Munich, Germany, October 13-15, 2003, pp. 153-158.